Comparison between left and right heart function in the isolated biventricular working rat heart

Gerhard Müller-Strahl MD[1], Jan Hemker MD[2],
Heinz-Gerd Zimmer MD PhD[2]

G Müller-Strahl, J Hemker, H-G Zimmer. Comparison between left and right heart function in the isolated biventricular working rat heart. Exp Clin Cardiol 2002;7(1):7-19.

OBJECTIVE: To provide a basic characterization of the crystalline perfused isolated rat heart preparation in its biventricular working mode.
ANIMALS AND METHODS: In 110 isolated biventricular heart preparations, flows and intraventricular pressures were examined by applying 24 and 28 different loading conditions to the left (LV) and right ventricle (RV), respectively.
RESULTS: LV and RV flows responded analogously to changes in loading conditions and were in accordance with the Frank-Starling principle. Linearization of parameters derived from the LV and RV function curves showed that the operation of both ventricles was quantitatively similar when unloaded and increasingly dissimilar when loaded. With increasing RV preload, the characteristics of the RV pump function curves changed; however, those of the LV hardly changed. Power, contractility and relaxation data of the ventricles were compared by applying the concept of corresponding afterloads, which showed that these parameters, except for power, had an inconsistent preload and afterload dependence in the LV and RV. Even though LV and RV performances displayed coexisting analogies, quantitative similarities and qualitative dissimilarities, in the case of relaxation, a concept unifying the heterogeneous data set for both ventricles has been developed. The hypothesis may be put forward that the macroscopic relaxation process of the heart muscle runs in parallel with cellular calcium handling.
CONCLUSIONS: At the level of the isolated denervated rat heart model, the common LV and RV functional parameters were only partially similar between the ventricles. However, a particular functional interdependence of relaxation data has been proposed to provide a unifying description of both LV and RV function.

Key Words: *Contractility; Isolated heart; Frank-Starling curves; Function curves; Pump function curves; Time constant of early relaxation; Ventricular mechanics*

[1]*Institut für Geschichte der Medizin, Ruhr-Universität Bochum, Bochum, and* [2]*Carl-Ludwig-Institut für Physiologie, Universität Leipzig, Leipzig, Germany*
Correspondence: Dr Gerhard Müller-Strahl, Institut für Geschichte der Medizin, Ruhr-Universität Bochum, Markstraße 258 A, 44799 Bochum, Germany. Telephone 49-234-32 28653, fax 49-234-32 14 205, e-mail gerhard.mueller-strahl@ruhr-uni-bochum.de

The original Langendorff heart preparation (1) had two major successors: the left ventricular (LV) working isolated rat heart (2) and the right ventricular (RV) working rat heart (3,4). There have been only a few attempts to combine these models in a single preparation (5,6), and it has not been characterized physiologically.

Even though the RV is of clinical relevance (7,8), there has been less emphasis on investigating RV function in the past. Furthermore, investigation of the functional differences between the entire LV and RV has been limited to a few in vivo studies where the control of inotropy by neural or humoral mechanisms is quite complex. An isolated heart preparation, however, would provide the ideal means to add to the insight obtained from these studies and those performed at an isolated muscular or cellular level (9,10). In this context, we were motivated to set up an isolated biventricular working rat heart preparation (IbiH) in which simultaneous acquisition of flow and intraventricular pressure would be feasible.

Our purpose was, first, to provide a basic characterization of this preparation and to establish a concept for the adequate comparability of the loading conditions of the LV and RV. To this intent, it has been shown that the LV and RV of the IbiH obey the Frank-Starling principle in an analogous manner. Parameters derived from the LV and RV function curves were linearized, leading to the finding that LV and RV operated similarly when unloaded and differed increasingly as their afterloads were increased. The flow data of the Frank-Starling curves were used to find corresponding afterloads of the LV and RV. For such afterloads, the power and parameters of contractility and relaxation of the ventricles were compared. Besides a complex quantification of related LV and RV data, which again showed coexisting similarities and dissimilarities of LV and RV function, a major finding of this latter analysis was that relaxation data of both ventricles could be interpreted by a unifying concept interrelating maximum ventricular pressure, rate of pressure decay and time constant of relaxation by a linear function. The hypothesis may be put forward that the macroscopic relaxation process of the heart muscle runs in parallel with cellular calcium handling. Therefore, the results of this investigation may be complementary to the abovementioned clinical findings and may help to explain the mechanical function of the heart muscle.

ANIMALS AND METHODS

Isolated biventricular working rat heart preparation

Two lots of female Wistar rats (83 in the first lot, 87±1.7 days old, weighing 229.8±2.6 g; and 27 in the second lot, 120±2.2 days old, weighing 258.1±1.5 g) were used for this study. Animals were maintained in a 12 h light plus 12 h dark cycle and given unlimited access to food (Altromin, Altromin GmbH, Germany) and water.

Animals were anesthetized with ether and thoracotomized. The heart was excised and arrested in ice-cold saline until subjected to retrograde perfusion with a modified Krebs-Henseleit bicarbonate buffer (116 mM NaCl, 3.7 mM KCl, 23.8 mM $NaHCO_3$, 1.25 mM $CaCl_2$, 1.18 mM KH_2PO_4, 0.6 mM $MgSO_4$, 5.5 mM glucose, 0.3 mM pyruvate and 5 U/l insulin, saturated with 95% O_2 and 5% CO_2, pH 7.4 to 7.45 at 37°C) (11) through an aortic cannula. In this Langendorff mode, the heart was perfused at a pressure of 90 cm H_2O. To complete this preparation, the large pulmonary vein, the pulmonary artery and the inferior vena cava were cannulated (the inner diameter of all cannulae was 1.8 mm). The remaining afferent vessels to the left and right atrium were ligated. Thus, in the IbiH, the atria were preserved and not used to receive the afferent cannulae.

The preparation was switched to the working mode by guiding the perfusion medium first through the left atrial cannula to the left heart (10 cm H_2O basic filling pressure), which ejected the fluid orthogradely against a hydrostatic load of 80 cm H_2O (left atrioventricular preparation) (12,13), and then through the vena cava cannula to the right heart (5 cm H_2O basic filling pressure), which ejected the fluid against a hydrostatic load of 15 cm H_2O (IbiH). These preloads and afterloads for the left and right heart were chosen because aortic and pulmonary artery flow were found to be identical under theses conditions. This situation is referred to as the basic loading condition of LV and RV. Perfusate, once ejected, did not recirculate. The isolated heart performed its pumping activity freely suspended in humid air at 37°C. The temperature was maintained by a Plexiglas chamber that closely surrounded the heart but that connected with the surrounding atmosphere.

Proximal to the semilunar valves, the aortic and pulmonary outflow tracts were each connected to a windkessel. The input impedances of the artificial pulmonary system and of the aortic system were adjusted according to the recommendations of Westerhof et al (14), with the sole difference that the resistive terms of the input impedances were varied by hydrostatic loading. It was verified that under these conditions the relation of pressure amplitude in the aorta to that in the LV corresponded to that in the in vivo situation (10).

Chemical agents

All chemicals used for the perfusate were reagent grade. Glucose was obtained from Merck (Germany), pyruvate from Serva (Germany) and insulin from Sigma (Germany). NaCl, KCl, $CaCl_2$, KH_2PO_4, $MgSO_4$ and $NaHCO_3$ were obtained from Roth (Germany). Carbogen (99.995%) was obtained from Messer Griesheim (Germany).

Data acquisition

Aortic flow and pulmonary artery flow were measured with an automated gravimetric method, and coronary effluate was collected at the pulmonary overflow after closure of a needle valve that controlled the inflow into the right atrium. Thus, the RV was unloaded, and only coronary effluate was supplying the RV with volume.

LV and RV transmural pressures were measured with semiconductor ultraminiature microtip pressure transducers (SPR-600, 5 µV/V/mmHg sensitivity, ±1% linearity,

>20 kHz natural frequency, 1.4 French tip, 1.3 French shaft traversing the valvular orifice; Millar Instruments, USA). Catheters were calibrated in a pressure chamber at 37°C. Catheter tips were inserted retrogradely into the respective ventricle. The catheter for the RV required a distal bend so that it fit the anatomical outflow tract specific for this ventricle. Pressure data were recorded and analyzed continuously. Selected fractions were transferred to a computer at a sampling frequency of 1 kHz (2 kHz for the second lot) for further data analysis. LV and RV peak pressures (LPmax and RPmax), LV and RV mean pressures, and the maximum and minimum of the first derivative of the respective ventricular pressure signals (LP′max, RP′max and LP′min, RP′min) were thus determined for the LV and RV, respectively. The temperature of the heart preparation was controlled with a type T thermocouple (0.41 mm diameter; Hugo Sachs GmbH, Germany) with its tip immersed in the aortic outflow laterally.

LV afterload (LVAL) and RV afterload (RVAL) were measured with a Statham DTXX pressure transducer (5 µV/V/mmHg sensitivity, ±1% linearity; Ohmeda GmbH, Germany). Preceding experiments had confirmed that the averaged aortic or pulmonary pressure signals thus obtained were equal to the averaged supravalvular pressure signals obtained with the extraventricular tip of a Millar double tip pressure sensor (SPR-467; same technical data as SPR-600). Second, it was confirmed that after averaging of these transducer signals, the afterloads equalled the hydrostatic pressure of the overflow system. Finally, it was verified that LV and RV outflow tracts shared the properties of Starling resistors.

Preloads were applied as filling pressures. At all loading conditions that were applied to the LV or RV of the IbiH, the end diastolic pressures measured in the respective ventricle were equal to the applied filling pressure. Therefore, the state of filling of the ventricles will be described by using the applied filling pressure.

Notation

LV and RV functions were first characterized on the basis of function curves. These curves described the dependence of the parameter, be it flow, mean (Pmean) or maximum (Pmax) intraventricular pressure, or the maximum (P′max) or minimum (P′min) of the first derivative of intraventricular pressure, on the preset preloads for a constant afterloading of the respective ventricle and for a standardized contralateral ventricle.

A group of function curves was denoted by L (left) or R (right), by a variable, x, representing any of the values in the respective range of preloads and by a value for the fixed afterload, for example, Lx,80. Eight groups of function curves were examined because eight afterloading conditions were applied. A group of function curves comprised several types of function curves. There were five types of function curves belonging to each group: for flow (Frank-Starling curve), Pmean, Pmax, P′max and P′min. Type of function curve was specified, when required, with an additional prefix indicating the functional parameter, for example, AFx,80, where AF is aortic flow.

Experimental protocol

After the preparation was switched from the Langendorff mode to the LV working heart (5 min) and successively to the biventricular mode (5 min), both ventricles of the isolated heart achieved a stable output after another 5 min under the basic loading conditions. During this period of stabilization, both catheters were inserted into the ventricles.

In the first series of measurements, RV preload (RVPL) and RVAL were kept constant at R5,15: standardized RV. LVAL was adjusted to a fixed value (50, 80, 110 or 140 cm H_2O), and LV preload (LVPL) was varied in steps of 5 cm H_2O (5, 10, 15, 20, 25 and 30 cm H_2O) every 5 min. At the end of each time interval, aortic flow, pulmonary artery flow, LP, RP, and aortic and pulmonary artery pressures were recorded. For LVPL less than 5 cm H_2O and LVAL of 140 cm H_2O, aortic flow dropped to zero. In this situation, the main portion of the cardiac output enters the coronary circulation. Therefore, 5 cm H_2O was taken to be the minimum preload and 140 cm H_2O the maximum afterload for the LV function curves. Since four LVALs were combined with six LVPLs, 24 loading conditions in total were examined to describe left heart function. In this series, 40 and 13 hearts were examined, respectively.

In the second series, LVPL and LVAL were kept constant at L10,80: standardized LV. A fixed RVAL was chosen (5, 10, 15 or 20 cm H_2O; 25 in some cases of the second lot). RVPL was varied in steps of 2.5 cm H_2O (2.5, 5, 7.5, 10, 12.5 and 15 cm H_2O) every 5 min. In the case of an interrupted inflow to the right atrium through the inferior vena cava cannula, the RVPL necessary for overcoming all of the above-indicated RVALs was observed to be 1 cm H_2O. Therefore, 1 cm H_2O was taken to be the minimum preload for the RV function curves. Since four to five RVALs were combined with seven RVPLs, a total of 28 to 35 loading conditions were examined to describe right heart function. In this series, 43 and 14 hearts were examined, respectively.

Because six preloads were applied to each ventricle, the respective preload ranges can be thought of as being subdivided into three pairs of preloads: low, medium and high preload ranges.

Measurements were made under basic loading conditions at the beginning, before any change in afterload and at the end of each experiment to assess the stability of the preparation.

Calculated parameters

The essential behaviour of any type of function curve was described by six parameters, as exemplified in Figure 1. If the preload was increased by 15 cm H_2O above the minimum preload, the resulting preload ranges (5 to 20 cm H_2O for the left and 1 to 15 cm H_2O for the right heart) were termed the standard preload ranges of the LV and RV. That these standard preload ranges were well defined is shown below (Results). By means of the standard preload range,

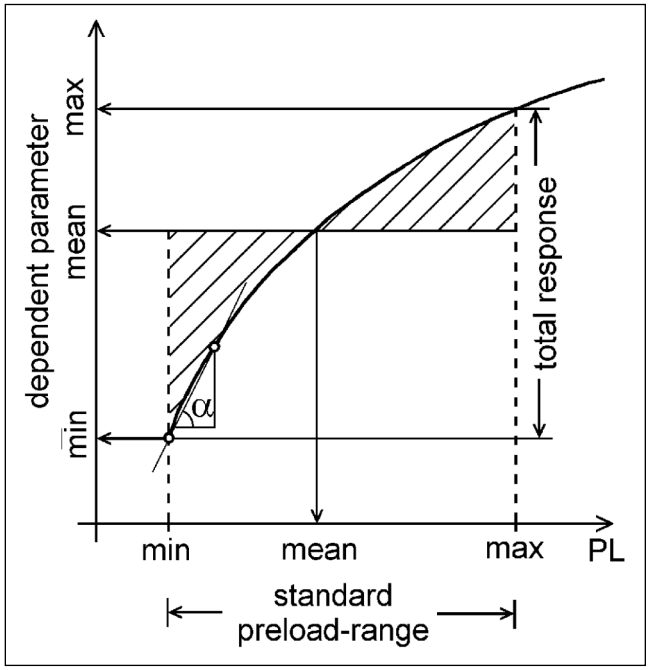

Figure 1) *General scheme for a function curve and its derived parameters. Preload (PL) was variable and afterload was kept constant. The contralateral ventricle was under standard loading conditions. For the ipsilateral-dependent parameter (flow, pressure) the minimum (min), mean and maximum (max) values were determined over the standard PL range. Total response was the range of response of the dependent parameter over the standard PL range. Initial slope was measured by tan α. Mean PL was determined from the mean value found for the dependent parameter*

the minimum, mean, maximum and total response values of the dependent parameter were determined (Figure 1). Furthermore, each mean value correlated with a mean preload (Figure 1). The slope between the two flows of the low preload range was termed the initial slope (Figure 1). It reflected the responsiveness of ventricular function in the low preload range.

Ejection time was derived from the pressure signal. The beginning ejection was placed 10 ms after P′max and the end ejection coincidentally with P′min. This procedure has commonly been used for the LV (15) but has also been shown to be transferable to the RV (16).

Pump function graphs have been shown to be useful measures of the ventricular state of contractility (17,18). These graphs represent the dependence of mean ventricular pressure on mean ventricular output and have been shown to be independent of flow variation, whether by an alteration in resistance or in arterial compliance. They reflect, however, any change in intrinsic cardiac contractility. A horizontal curve reflects a pump that generates pressure, and an infinite, steep curve reflects one that generates flow.

External cardiac power was determined as pressure-volume work per unit time (19,20). For any given afterload, a preload was determined where the external power of the respective ventricle was maximal. Maximum power of the RV was normalized to free RV weight and that of the LV to free LV weight plus septal weight.

For the LV and RV, indexes of contractility (LIC and RIC, respectively) were calculated for each afterload as the slopes obtained from linear regression analyses of the LV and RV data, respectively, entered into a P′max-Pmax plot. The LV and RV indexes of relaxation (LIR and RIR, respectively) were calculated for each afterload as the mean of the –P′min to Pmax ratios for LV and RV data, respectively.

The time constant of early relaxation of pressure, T, was determined by the derivative method (21): T was obtained from the superposition of data of 25 beats, which underwent linear regression analysis in a semilogarithmic P′-P plot.

Comparison between LV and RV function

The synchronous activity of both atria and both ventricles in one preparation allowed for a functional comparison of LV and RV according to the following methods. Minimum, mean and maximum values of the function curves are parameters that offer the possibility to observe the behaviour of any type of function curves versus afterload and to compare absolute values obtained from the LV and RV. It will be shown below that the concept of mean flow supports the concept of corresponding afterloads of LV and RV: corresponding afterloads of the LV and RV were those for which the respective mean flows were identical.

Total response allows for a comparison of all types of function curves of one group, of different groups and of both sides of the heart because it represents the range of variability of the dependent parameter over the standard preload range, irrespective of the type of parameter.

By applying the concept of corresponding afterloads, LV and RV powers, LIC and RIC, and T of LV and RV were compared.

Statistical analysis

Standard methods were used to calculate mean values, SEM and the relative coefficient of variation (V_r). Mean values were compared using the two-tailed *t* test for paired and unpaired samples after confirming the normal distribution of data (Q-Q plot and Kolmogorov-Smirnov test) and the similarity of their variances. Linear regression analysis was based on the method of least square fitting. One-way analysis of variance (ANOVA) was applied after confirming the homogeneity of variance according to Levene; differences between subgroups were evaluated according to the Student-Newman-Keuls test and Tukey's HSD procedure. Tests were performed with SPSS for Windows, version 6.1.3 (SPSS Inc, USA). A level of significance of 0.05 was used in all tests. All values are presented as mean ± SEM.

RESULTS

Heart weights, heart rate and ejection time

The average heart weight was 0.79±0.01 g for the total population (n=110). The average free LV weight was 0.38±0.01 g, free RV weight was 0.15±0.01 g, and septal weight was 0.19±0.01 g. The respective values for hearts of the first and second lot and for hearts of the first and second series did not differ significantly.

TABLE 1
Stability of the isolated biventricular working rat heart preparation

Time (min)	AF (mL/min)	LPmax (mmHg)	PF (mL/min)	RPmax (mmHg)	CF (mL/min)
0 (n=83)	31.8±0.69	84.3±0.70	30.3±0.47	35.8±0.56	8.2±0.17
35 (n=83)	31.8±0.90	83.9±0.57	29.4±0.55	35.3±0.67	7.8±0.17
70 (n=32)	27.3±1.52	82.5±0.84	24.8±0.86	33.6±1.08	6.7±0.24

At the indicated times after the initial measurement, control runs were performed with the heart under basic loading conditions. Data are mean ± SEM. AF Aortic flow; CF Coronary flow; LPmax Left ventricular peak pressure; PF Pulmonary artery flow; RPmax Right ventricular peak pressure

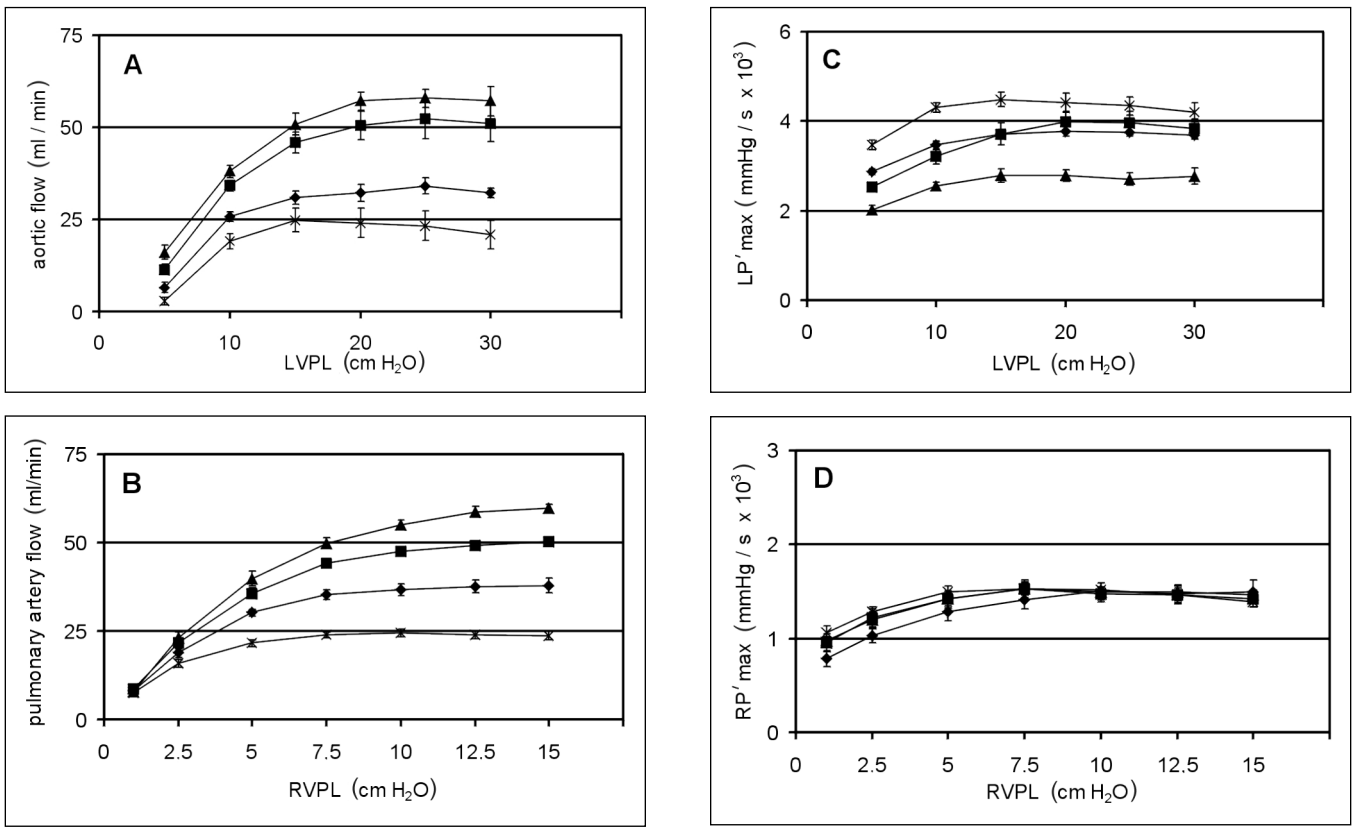

Figure 2) *Types of Frank-Starling curves for the left (LV) and right ventricles (RV). (A) Aortic flow types: AFx,50 (▲, n=10), AFx,80 (■, n=11), AFx,110 (◆, n=10) and AFx,140 (×, n=13). (B) Pulmonary artery flow types: PFx,5 (▲, n=10), PFx,10 (■, n=13), PFx,14 (◆, n=10) and PFx,20 (×, n=13). (C) LV pressure types: LP´max x,50 (▲, n=10), LP´max x,80 (■, n=11), LP´max x,110 (◆, n=10) and LP´max x,140 (×, n=13). (D) RV pressure types: RP´max x,5 (▲, n=10), RP´max x,10 (■, n=13), RP´max x,15 (◆, n=10) and RP´max x,20 (×, n=13)*

The spontaneous heart rate was 5.22±0.02 beats/s on average (n=110, V_r=0.36). This justified the assumption that the frequency was constant in the hearts used in this study. For that reason, all flow data within this study may be interpreted equivalently as stroke volumes.

The ejection time was found to be 66.7±0.57 ms on average (n=60) and to be independent of afterload and preload. Furthermore, it was independent of the side of the heart (ANOVA).

Stability of the preparation and flows under basic loading conditions

When control flow data were pooled, no significant changes of the measured flows were detected during the first part of the experiments. In the second part, aortic flow, pulmonary artery flow and coronary effluate decreased slightly, but not significantly (Table 1). Furthermore, aortic flow and pulmonary artery flow were equal during the entire course of the experiments. The pressure parameters did not decrease at all during the experiments (see, for example, Pmax in Table 1) (ANOVA).

Frank-Starling curves and corresponding function curves

Figure 2 shows representative types of Frank-Starling curves for the left and right heart. The function curves displayed an asymptotic behaviour, the asymptote being parallel to the preload axis. The response of aortic flow and pulmonary artery flow (Figure 2A,B) to an equally stepped change in preload was greatest for smaller preloads and flattened when the highest preload was approached. No 'descending limbs'

TABLE 2
Flow and pressure parameters for four groups of Frank-Starling curves for the left ventricle at varying preloads and afterloads (Lx,n) and with the right ventricle preloaded at 5 cm H_2O and afterloaded at 15 cm H_2O (R5,15)

Loading conditions of both ventricles (cm H_2O)	Preload	AF (mL/min)	LPmax (mmHg)	LPmean (mmHg)	LP′max (mmHg/s)	LP′min (mmHg/s)
R5,15, Lx,50, n=10,	Minimum	16.10±1.97	50.00±1.37	17.34±0.49	2202±103	–1512±100
PLmean=10.79±0.27	Maximum	57.11±2.42	65.26±1.51	25.58±0.89	2785±127	–1477±80
	Mean response	40.53±1.78	60.25±1.04	21.83±0.63	2536±102	–1609±84
	Total response (%)	267.77±49.54	31.52±4.87	47.78±3.99	39.99±7.77	–0.48±5.15
	Initial slope (mL/cm H_2O)	4.38±0.25				
R5,15, Lx,80, n=11,	Minimum	11.45±1.52	71.75±1.12	28.33±0.86	25.19±104	–2266±143
PLmean=10.39±0.29	Maximum	50.48±3.83	89.58±2.09	37.39±0.73	3987±232	–2577±108
	Mean response	35.52±2.20	83.09±1.47	32.80±0.82	3358±174	–2500±109
	Total response (%)	337.73±38.28	24.87±2.37	32.64±2.36	58.08±6.63	–16.67±5.84
	Initial slope (mL/cm H_2O)	4.55±0.22				
R5,15, Lx,110, n=10,	Minimum	6.56±1.37	94.28±1.54	40.05±1.13	2874±68	–2424±98
PLmean=9.60±0.16	Maximum	32.20±2.28	106.58±1.49	47.51±0.94	3769±111	–3084±57
	Mean response	23.87±1.34	102.88±1.04	44.14±0.88	3455±80	2935±61
	Total response (%)	515.94±102.34	13.21±1.63	19.08±2.00	31.46±3.67	29.27±5.65
	Initial slope (mL/cm H_2O)	3.83±0.22				
R5,15, Lx,140, n=13,	Minimum	2.86±0.96	113.45±1.68	49.36±1.47	3468±110	–3088±127
PLmean=9.65±0.27	Maximum	24.01±4.03	123.38±1.36	58.01±1.33	4416±206	–3552±134
	Mean response	17.66±2.49	120.97±1.03	54.39±1.17	4168±133	–3522±117
	Total response (%)	586.53±118.68	8.95±1.46	18.42±3.59	27.36±4.14	15.58±2.45
	Initial slope (mL/cm H_2O)	3.22±0.29				

Data are mean ± SEM. AF Aortic flow; LPmax Left ventricular peak pressure; LPmean Left ventricular mean pressure; LP′max Maximum of the first derivative of left ventricular pressure; LP′min Minimum of the first derivative of left ventricular pressure; PLmean Mean preload

for either LV or RV function curves were found. This asymptotic behaviour of the flows was reflected in pressure data (Pmean, Pmax or P′max) to a lesser degree, however (for example, Figure 2C,D compared with Figure 2A,B), so that for medium and high preloads the pressure parameters were already close to the asymptote.

The results of all groups of function curves are summarized in the Tables 2 and 3 for the left and right heart, respectively. In these tables, each of the eight groups of function curves is indicated in the first column by the symbols for the loading conditions. Within each group, the total response of flow was by far greater than the total response of any other parameter (Tables 2,3). The mean flow of the LV (35.5±2.2 mL/min; Lx,80; x=5, ... , 20) was not significantly different from the flow under basic loading conditions (31.8±0.78 mL/min; L10,80), nor was the mean flow of the RV (29.2±1.2 mL/min; Rx,15; x=1, ... , 15) different from the flow under basic loading conditions (30.3±0.5 mL/min; R5,15). These results support the choice of the standard preload ranges. As a consequence, the mean preloads of LV (10.4±0.3 cm H_2O, LVAL=80; Table 2) and RV (4.8±0.1 cm H_2O; RVAL=15; Table 3) were not significantly different from their respective standard preloads of 10 and 5 cm H_2O. Furthermore, for afterloads that were different from the standard afterloads, the mean preloads of the LV and RV did not differ significantly from their standard preloads of 10 and 5 cm H_2O (Tables 2,3). These findings further confirmed the choice of the standard preload ranges.

DISCUSSION

Function curves of LV and RV and the linearization of their parameters

Continuity of flow between RV and LV: Data from Figure 2 were used to consider the potential balance of pulmonary artery flow and aortic flow when RVAL and LVPL were set to be equal (common load). Four cases may be distinguished. First, for a common load of 5 cm H_2O, RVPL of 2.5 cm H_2O delivered a pulmonary artery flow sufficient to supply the LV with the necessary flow for all LVALs (when RVPL was 1 or greater than 2.5, the RV output was either too small or too large with respect to the LV flow). Second, when the common load was set to 10 cm H_2O, the necessary RVPLs were 2.5 to 7.5 cm H_2O to supply the LV at all LVALs (there was a lack or surplus of RV flow relative to LV flow for RVPL less than 2.5 or greater than 7.5, respectively). Third, for a common load of 15 cm H_2O, RVPLs of 7.5 to 15 cm H_2O were needed to supply the LV with the necessary flow for the LVALs 80, 110 and 140 cm H_2O (when LVAL is 50 cm H_2O, the left heart can potentially transport

TABLE 3
Flow and pressure parameters for four groups of Frank-Starling curves for the right ventricle at varying preloads and afterloads (Rx,n) and with the left ventricle preloaded at 10 cm H_2O and afterloaded at 80 cm H_2O (L10,80)

Loading conditions of both ventricles (cm H_2O)	Preload	PF (mL/min)	RPmax (mmHg)	RPmean (mmHg)	RP′max (mmHg/s)	RP′min (mmHg/s)
Rx,5, L10,80, n=10,	Minimum	7.65±0.34	13.56±0.83	5.66±0.97	787±87	–534±83
PLmean=5.33±0.17	Maximum	59.62±1.19	34.84±2.63	17.13±0.89	1494±125	–1001±85
	Mean response	41.95±1.05	28.94±1.72	12.88±0.75	1284±85	–918 ±82
	Total response (%)	694.51±38.78	157.74±12.20	260.94±40.82	103.20±19.09	104.75±15.70
	Initial slope (mL/cm H_2O)	6.12±0.76				
Rx,10, L10,80, n=13,	Minimum	8.50±0.42	23.84±1.51	9.08±0.58	955±96	–712±67
PLmean=5.13±0.14	Maximum	50.35±0.94	36.15±1.67	17.19±0.69	1417±85	–952±53
	Mean response	38.70±0.90	34.69±1.59	15.30±0.67	1347±87	–954±56
	Total response (%)	511.08±32.34	55.60±6.71	96.92±11.42	55.93±7.11	41.06±7.51
	Initial slope (mL/cm H_2O)	5.27±0.49				
Rx,15, L10,80, n=10,	Minimum	8.19±0.38	26.40±1.08	10.23±0.72	980±38	–835±37
PLmean=4.81±0.14	Maximum	37.88±2.08	36.09±1.99	17.35±1.28	1466±51	–952±48
	Mean response	29.23±1.19	34.87±1.52	16.11±0.96	1367±55	–962±44
	Total response (%)	364.69±20.02	37.73±6.81	72.81±9.59	50.54±4.68	15.02±5.68
	Initial slope (mL/cm H_2O)	4.26±0.47				
Rx,20, L10,80, n=13,	Minimum	7.50±0.38	30.68±1.41	13.58±0.82	1055±75	–826±38
PLmean=4.18±0.24	Maximum	23.68±1.24	35.45±1.29	18.12±1.14	1391±58	–805±35
	Mean response	20.10±0.85	36.53±1.31	17.88±0.92	1390±60	–877±37
	Total response (%)	228.48±25.86	17.11±4.43	36.92±8.96	41.38±13.56	–1.34±4.25
	Initial slope (mL/cm H_2O)	3.33±0.51				

Data are mean ± SEM. PF Pulmonary artery flow; PLmean Mean preload; RPmax Right ventricular peak pressure; RPmean Right ventricular mean pressure; RP′max Maximum of the first derivative of right ventricular pressure; RP′min Minimum of the first derivative of right ventricular pressure

more volume than can be supplied by the right heart). Fourth, when the common load was set to 20 cm H_2O, the output of the RV with an RVPL set to 7.5 to 15 cm H_2O was sufficient just for the LV afterloaded at 140 cm H_2O; for LVAL less than 140 cm H_2O, the transport through the RV was too small relative to that through the LV. In summary, the following rule was deduced: the higher the common load, the higher RVPL and LVAL had to be to guarantee continuity of flow through the RV and LV. To decrease RVPL or LVAL in a situation of established continuity would lead to a mismatch between the flows in series.

Frank-Starling mechanism for the IbiH: In early studies of the Frank-Starling principle (22,23), preload was applied as volume load or – in more recent studies – with an isovolumetric contralateral ventricle. A constant contralateral volume load means constant contralateral diastolic compliance and, as a consequence, the ipsilateral end diastolic pressure-volume relation remains unaltered. However, in the IbiH the contralateral filling pressure was kept constant; this shifted the ipsilateral pressure-volume relation toward the right. From Tables 2 and 3 and Figure 2A,B it can be concluded that, for increasing preload, the function curves for flow express the phenomenon typically predicted by the Frank-Starling principal. Another aspect is that, for a given preload, an increase of afterload led to a reduction of ventricular output (Figure 2A,B). Taken together, LV and RV obeyed the Frank-Starling principle. In this regard, both ventricles operated analogously.

Linearization of LV and RV flow parameters and the concept of corresponding afterloads of LV and RV: There have been several attempts to linearize ventricular function over either preload (15,18) or afterload (20,24). For the IbiH, certain information can be derived from the LV and RV function curves; these parameters changed linearly with a change in afterload.

Minimum, mean (Figure 3A) and maximum aortic flow (Table 2) decreased linearly with increasing LVAL ($0.62>r^2>0.52$). Theoretically, for LVAL=0, the minimum, mean and maximum aortic flow would be 23, 54 and 78 mL/min, respectively. Minimum, mean and maximum aortic flow became zero for the theoretical afterloads of 157, 205 and 199 cm H_2O.

The minimum pulmonary artery flow of the right heart (a value close to that of the coronary effluate) was a constant function of RVAL ($V_r<2.6\%$); this indicated that coronary effluate was transported by the right heart against any RVAL, showing that the RV has an expedient mechanism. Mean (Figure 3A) and maximum values of pulmonary artery flow were approximated linearly, however ($0.89>r^2>0.85$), and were inversely related to RVAL

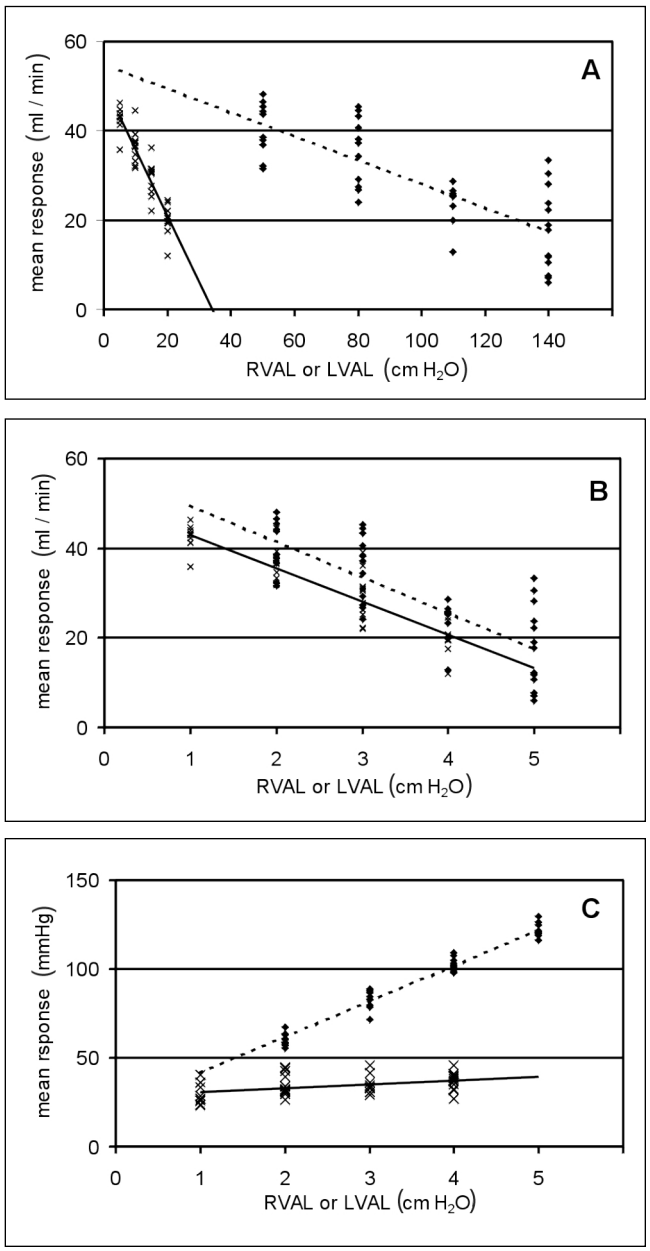

Figure 3) *Linearization of left (LV) and right ventricular (RV) mean responses over afterload (AL). (A) Mean responses of aortic flow (AF) (◆; dashed line) and pulmonary artery flow (PF) (×; solid line) over one common AL axis. Mean PF decreased 5.5 times mean AF. LVAL Left ventricular afterload; RVAL Right ventricular afterload. (B) Mean responses of AF (◆; dashed line) and PF (×; solid line) after overlaying the LVAL axis with the transformed RVAL axis. A change by one arbitrary unit on the new axis represents a change of LVAL by 30 cm H_2O and RVAL by 5 cm H_2O. (C) Mean responses of LPmax (◆; dashed line) and RPmax (×; solid line). Same AL axis as in panel (B). Increasing activation of LPmax with increasing LVAL was responsible for the delayed decline of mean AF in panel (A)*

(Table 3). For a theoretical RVAL=0, minimum, mean and maximum pulmonary artery flow was 8.3, 50 and 73 mL/min. Mean and maximum values were comparable with those for the LV. This was an indicator that LV and RV functioned similarly because the afterload free state (LVAL=RVAL=0) allowed for an afterload-independent comparison of the ventricular functions. The theoretical RVALs where mean and maximum pulmonary artery flow ceased were 34 and 30 cm H_2O, respectively. These values were low in contrast to the corresponding LVALs. This was an indicator of dissimilarity between RV and LV.

Next, linearization of flow over afterload opened a natural way to find corresponding afterloads of the LV and RV: the RVAL axis had been transformed such that the RV slope for mean flow as a function of afterload became identical to that of LV mean flow. A good agreement was achieved under the assumption that a change in LVAL of 30 cm H_2O corresponded to a change in RVAL of 5 cm H_2O (Figure 3B). Because the afterloads 80 and 15 cm H_2O had already been shown to correspond, the remaining corresponding pairs of afterloads were 50 and 10, 110 and 20 and, for the second lot of IbiH, 140 and 25 cm H_2O. There was no corresponding LVAL for RVAL of 5 cm H_2O.

Linearization of LV and RV pressure parameters: Minimum, mean (Figure 3C) and maximum values of LPmax were directly related to LVAL ($0.97>r^2>0.93$); the same was valid for the minimum value of RPmax ($r^2=0.53$). The mean and maximum values of RPmax (Figure 3C) were constant ($V_r<3.1\%$), however. For LVAL of 0 cm H_2O, the theoretical LPmax was 15, 28 and 36 mmHg (minimum, mean and maximum, respectively). Comparable values were found for the RV: 10.7, 28 and 35 mmHg, respectively. This finding for the afterload-independent situation again indicated similarity between both ventricles. The theoretical minimum, mean and maximum values of LPmax that were calculated for the theoretically maximum LVAL was 137, 165 and 162 mmHg, respectively. For the RV, in contrast, the corresponding minimum value of RPmax was found to be 43 mmHg, indicating a dissimilarity between the LV and RV. The relations found between Pmean and afterload were analogous to the above analysis of the Pmax values.

The minimum and mean values of LP′max were linearly dependent on LVAL and displayed a positive correlation ($0.72>r^2>0.60$). The maximum values of LP′max and the minimum, mean and maximum values of RP′max were constant functions over RVAL ($V_r<4.5\%$). There was an inverse interdependence between minimum, maximum and mean LP′min and LVAL ($0.80>r^2>0.63$) and a constant between minimum, mean and maximum RP′min and RVAL ($V_r<4.6\%$). For P′max and P′min at an afterload of 0 cm H_2O, again, LV and RV were similar; their properties of contraction or relaxation, however, diverged with increasing afterload.

Adaptation of flow and pressure parameters to afterload: Putting together the results for the minimum, mean and maximum values of flow and pressure data, the pressure parameters of the LV adapted in a direct proportional fashion with increasing LVAL (Figure 3C), and this led to a delayed inverse adaptation of aortic flow to LVAL (Figure 3A). Nevertheless, LV pressure adaptation was not sufficient to compensate for LV loss of function with respect to flow. In contrast, the pressure parameters of the RV hardly adapted (Figure 3C). This led to a marked inverse adaptation of pul-

monary artery flow to RVAL (Figure 3A). Therefore, the RV was much more sensitive than the LV to corresponding afterload changes. The results presented for the LV are in agreement with earlier studies (25) in which a cooperative activity of cross-bridge formation in response to afterload elevation was postulated to explain the pressure response of cardiac muscle to increased LVAL. Thus, the conclusion is justified that RV may lack such a cooperative activity. Another concept similar to that of cooperative activity is that of afterload reserve (26), which differs from the former in so far as it does not directly refer to the cross-bridge mechanism but to the increase of P′max or –P′min with increasing afterload. Thus, the conclusion is justified that LV and RV differ in that the LV has a much higher afterload reserve than the RV. In summary, the LV appeared to adapt to changing afterload conditions, whereas the RV built up pressure always to the same degree regardless of RVAL; RV output appeared to be regulated passively by the change in RVAL.

Response of ventricular function to preload and its relation to afterload: The total response of aortic flow (Table 2) was nearly independent of LVAL (V_r=9.2%), whereas that of pulmonary artery flow (Table 3) decreased with RVAL (r^2=0.73). At an afterload of 0 cm H_2O, the total response of pulmonary artery flow was 11 times that of aortic flow, which vanished, however, at an RVAL of about 35 cm H_2O. The total responses of Pmax and Pmean for the LV and RV decreased with increasing afterload ($0.65>r^2>0.48$). However, the decrease was 3.8 and 4.6 times faster, respectively, for the RV. At an afterload of 0 cm H_2O, the total response of RPmax was 3.8 times that of LPmax. The total responses of P′max and P′min remained constant with changes in afterload ($18.8\%>V_r>8.7\%$) irrespective of the side of the heart. These data show that the LV not only actively compensated for an increase of afterload but also maintained the range of response to preload. This characterization differs from that of the RV, which lost the range of response to preload with increased RVAL. At low afterloads, however, the RV range of response was significantly higher than that of the LV.

In addition to total response, initial slope (Tables 2,3) was a parameter used to estimate the response of a ventricle to a change in preload in the lowest of the preload ranges. For LV and RV, no clear dependence of these slopes on afterload was found (ANOVA). Therefore, data from to one ventricle were pooled. The RV (4.7±0.32 mL/cm H_2O; n=46) was found to be 1.2 times ($P<0.05$) more responsive than the LV to changes in ipsilateral preload (3.96±0.15; n=44).

Comparison between LV and RV functions according to their pump function curves

There is one drawback to the use of function curves as indicators of myocardial contractility: pumping characteristics of the LV and RV appear to depend on preload and afterload. The dependence on afterload can be eliminated by the construction of pump function curves (Figure 4). To our knowledge, the pump function graphs in Figure 4 are the first obtained for isolated working rat hearts. At minimum preload (LVPL of 5 cm H_2O), the LV pump function curve is linear. Its position within the graph reflects a behaviour intermediate between flow generator and pressure generator. With increasing preload, the LV pump function graph underwent first a parallel shift (standard LVPL of 15 cm H_2O) and then a shift plus a slight rotation toward a horizontal position (maximum LVPL of 20 cm H_2O). Such changes are interpreted as being typical of increased end diastolic filling (18). In contrast, the RV pump function curve underwent a

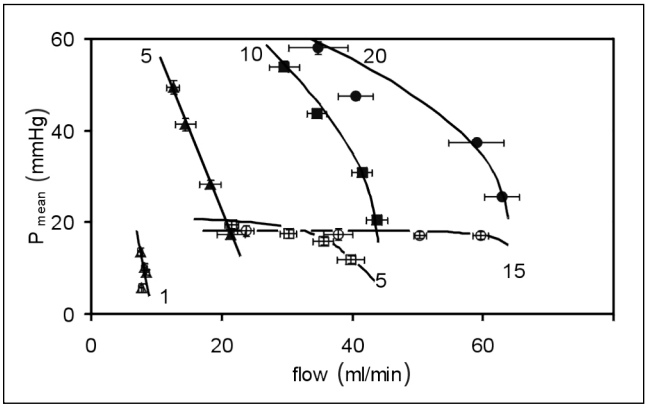

Figure 4) *Pump function curves for the left (LV) and right ventricle (RV). Mean pressure (Pmean) is plotted over flow for each ventricle at each afterload. The points belonging to one afterload are joined to a pump function curve by a nearly linear relation. Each pump function curve expresses one state of contractility. With a change of preload, the curves shift or rotate. Filled symbols refer to the LV (LV afterload 50, n=10; 80, n=11; 110, n=10; and 140 cm H_2O, n=13) and unfilled symbols to the RV (RV afterload of 5, n=10; 10, n=13; 15, n=1; and 20 cm H_2O, n=13). Triangles indicate minimum, squares standard and circles maximum preloads for the respective ventricles*

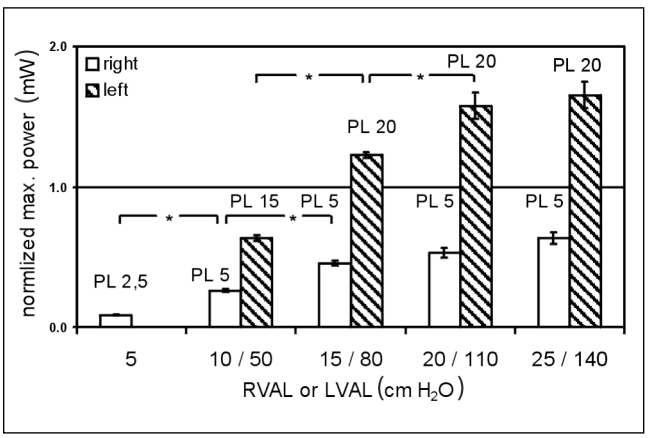

Figure 5) *Comparison between left (LV) and right ventricular (RV) normalized maximum power at corresponding afterloads. Power was preload (PL) dependent for both ventricles. Bars represent the power of the respective ventricle at the PL where the power was found to be maximal. For LV and for RV there was an analogous dependence on LV afterload (LVAL) and RV afterload (RVAL), respectively. Asterisked brackets indicate significant differences (n=9 at 140, n=8 at 15, n=7 at 110 and 140 cm H_2O, and n=6 for all others)*

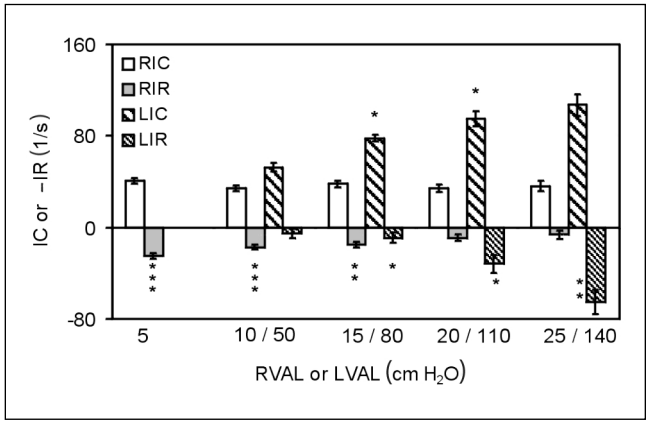

Figure 6) *Comparison between left (LIC) and right indexes of contractility (RIC) and negative left (–LIR) and right indexes of relaxation (–RIR) at corresponding afterloads. LIC and RIC were found to be independent of the applied preload. RIC and RIR were independent of RV afterload (RVAL). In contrast, LIC and LIR were afterload dependent. One or two asterisks associated with one LV column indicate a significant difference from the first or second LV column to the left. Two or three asterisks associated with one RV column indicate a significant difference from the second or third RV column to the right (n=9 at 140, n=8 at 15, n=7 at 110 and 140 cm H_2O, and n=6 for all others)*

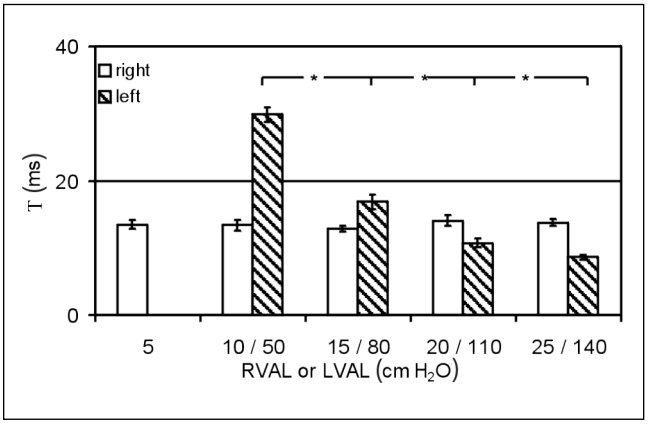

Figure 7) *Comparison of the time constant of early relaxation of ventricular pressure (T) for the left (LV) and right ventricles (RV) at corresponding afterloads (ALs). Because for the medium and high preload (PL) ranges T was not dependent on PL, data for these PLs were pooled and are displayed for corresponding ALs. T of RV did not change with RVAL and was of the same size as T of LV at standard LVAL. T of LV adapted strikingly to an increase of LVAL from 50 to 80 cm H_2O. This adaptation led to a decrease of T with each AL increment (n=5 at all ALs, except n=7 for AL of 25 cm H_2O)*

complete transformation on shifting with increasing RVPL: first, it was infinitely steep (RVPL of 1 cm H_2O), then it inclined moderately (RVPL of 5 cm H_2O) and, finally, it was completely horizontal (RVPL of 15 cm H_2O). Therefore, at minimum RVPL, the RV was a pressure generator and at maximum RVPL a flow generator. This rotation of the RV pump function can be ascribed to an increase of the inotropic state (18) and has been described in this investigation for the first time. It is concluded that LV and RV pumps operate analogously for the RVPL range of 1 to 5 cm H_2O and the LVPL range of 5 to 20 cm H_2O (qualitative similarity and quantitative dissimilarity); the RV shows a particular behaviour at high RVPL (qualitative dissimilarity).

Comparison between LV and RV functions according to the concept of corresponding afterloads

Normalized maximum power: For corresponding afterloads, the normalized maximum power of the LV was about 2.5 to 3 times that of the RV (Figure 5). For the RV, this parameter increased continuously with RVAL, though not significantly beyond RVAL of 15 cm H_2O. An analogous afterload dependence was found for the LV power that plateaued beyond LVAL of 110 cm H_2O. The results for LV agree with earlier studies (22,27,28). Additionally, it was found that the RV power showed an analogous behaviour.

LV and RV indexes of contractility and relaxation: For any fixed afterload, P′max correlated well with Pmax ($0.95>r^2>0.75$ for LVALs and $0.85>r^2>0.52$ for RVALs). Thus, the slopes of these correlations, LIC and RIC, were measures of contractility independent of preload at any fixed afterload. However, LIC depended significantly on afterload in that contractility linearly ($r^2=0.85$) increased with increased LVAL (Figure 6). In contrast, RIC was independent not only of RVPL but also of RVAL (Figure 6). LIC was on average 1.6 to 3 times greater than the RIC at corresponding afterloads.

LIR was linearly ($r^2=0.53$) related to LVAL, whereas RIR was independent of RVAL (Figure 6). At the corresponding afterloads of the standard loading conditions, LIR and RIR were about the same; for the remaining corresponding afterloads, LIR was 0.8 to 1.3 times RIR.

To summarize, LIC and LIR adapted to afterload in a manner that would be advantageous for LV ejection and filling; RV data indicated that RIC is not adapted to RVAL and even that RIR is slightly deteriorated. RV contractility can be characterized by a sole RIC and sole RIR, which were preload and afterload independent. The average RIC was about 1.4 times the average RIR. Thus, there was a striking dissimilarity between LV and RV contractility data.

In the past, contractility and relaxation indexes were frequently used as measures of contractility and relaxation (for example, 29). They were thought to reflect a strict coupling of mechanical events at different periods of the cardiac cycle. It was only in the case of LV indexes (Figure 6) that this coupling changed with LVAL. The corresponding RV indexes did not show this adaptation to RVAL. The findings for LIR agree with earlier studies (30,31) in which LP′min was found to depend on LPmax. Additionally, the findings of these studies for the LV were confronted with our findings which revealed a dissimilar way of RV operation.

Time constant T of early relaxation: T of LV and RV were dependent on preload only within the lower preload range (data not shown). Therefore, for each afterload, the data concerning the medium and higher section of the preload ranges were pooled (Figure 7). T of the LV depended on

LVAL, but T of the RV did not depend on RVAL, a qualitative dissimilarity. At standard loading conditions, T of the LV and RV were identical, a quantitative similarity. At the corresponding afterloads of 10 and 50 cm H_2O, T of LV was twice that of RV; at the corresponding afterloads of 25 and 140 cm H_2O, T of LV was nearly half the corresponding T, a quantitative dissimilarity.

Unifying concept of LV and RV phases of relaxation

The obvious inconsistent dependence of the different classical measures of relaxation on LVAL and RVAL (Figures 6,7) stimulated the search for an afterload- and preload-independent parameter unifying the description of LV and RV relaxation processes. For this purpose, 1/LIC and 1/RIC were plotted versus their respective T's (Figure 8). LV values were clearly linearly related (r^2=0.8; P<<0.001) with a slope close to unity (0.85±0.05). Alternatively, this linear relation can be described sufficiently by two parameters: 1/LIRmax, defined as the value at the intersection with the 1/LIR axis where LIR is maximal, and –1/k, defined as the value at the intersection with the T axis and k being a constant; these definitions yield the equation 1/LIR = (k/LIRmax) T + (1/LIRmax). That there was a saturation process hidden behind this equation was shown by solving it for LIR: LIR = LIRmax / (k T + 1), in which LIR approaches the T axis asymptotically for large T.

Interpretation of the corresponding plot of RV data was straightforward as well: no linear relation was found because RV data accumulated in a circumscribed field within the plot (bars in Figure 8). These RV data were essentially part of the relation found for the LV. This behaviour of the RV data was understood to result from similar proportional balances between the parameters of relaxation of LV and RV, respectively, and, on the other hand, from a differing mode of their regulation. For example, if LVAL is increased, then the necessary increase of LPmax is intimately coupled with a decrease of LP′min and a prolongation of T; thus, the regulated state of LV relaxation parameters, as described by the linear regression line in Figure 8, is maintained. Such regulatory mechanisms are quite limited for RV relaxation. In other words, the linear relation between 1/LIR and T of LV reflects a controlled interdependence of different elements of the relaxation phase, of LPmax, LP′min and T. RV data can be superimposed on LV data (quantitative similarity) but cover only a narrow section of the latter (qualitative dissimilarity).

Finally, to show the utility of the proposed concept, we hypothesized that the saturation kinetics expressed in the 1/LIR-T graph (Figure 8) indicates the response of the whole LV, reflecting cellular mechanisms. For this purpose, the index of relaxation was identified with the velocity of pressure decay that, on the cellular level, had been shown previously to be linked to the rate of calcium removal from the cytosol by the sarcoplasmic reticulum (32). T was considered to be an inverse measure of cytosolic calcium concentration because the collective calcium pump activity increases with increasing calcium concentration (33); an increase of calcium pump activity was assumed to reduce T.

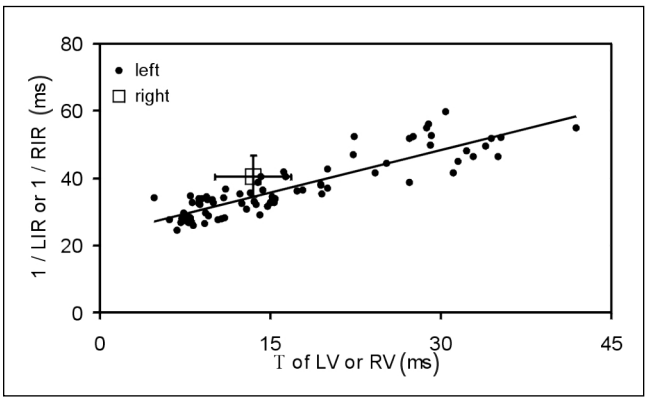

Figure 8) *Linear relation between the parameters of left (LV) and right ventricular (RV) relaxation processes. Regardless of the respective ventricular loading condition, the inverse left (1/LIR) and right indexes of relaxation (1/RIR) were plotted versus the time constant of early relaxation of ventricular pressure (T) of the LV or RV. LV data were fitted to a linear function (r^2=0.8, P<0.001). The slope of the linear regression is a dimensionless, LV preload (LVPL) and LV afterload (LVAL) -independent characteristic measure of LV function. RV data entered into the graph coincided with the line of regression for LV data. However, because RV data accumulated within a circumscribed area, the latter are represented by the crossed bars (mean ± SEM). Thus, the coexistence of similar and divergent properties of LV and RV relaxation are shown (n=5 at all ALs, except n=7 for AL of 25 cm H_2O)*

This rationale led to the Lineweaver-Burk plot describing enzyme kinetics according to the following equation: LIR = LIRmax $[Ca^{2+}]/(K + [Ca^{2+}])$, where K is a constant and LIRmax represents the asymptote for a large $[Ca^{2+}]$. Furthermore, LV and RV collective calcium pump activities were interpreted as being identical under standard loading conditions (quantitative similarity), in agreement with studies on myocytes (33). However, the response to load in the LV was regulated differently from that in the RV (qualitative dissimilarity). To our knowledge, investigations comparing LV and RV myocytes from this point of view of relaxation have not been published.

Comparison with the literature

LV contractility and relaxation data have been largely discussed in the literature. We have shown that our results correspond with those in the literature for the case of the LV. The corresponding problems for the entire isolated RV have been sparsely discussed in the literature, however. Therefore, it was of interest to compare our results for the RV of the IbiH with published data from closely related preparations.

Our findings confirmed that relaxation of the right myocardium (34) should be completely independent of afterload for the entire RV, in contrast to other studies of in situ heart preparations showing that RV relaxation depends on afterload after pharmacological blockade with atropine and propanolol (35) in the isolated RV myocardium (31,36) or in myocytes originating from the RV (37).

Zile and co-workers (38) found that an increase in preload did not influence the time course of either LV or RV relaxation of isolated cardiac muscle. Because these authors had examined 30% to 100% of the preload range, these

results might be reconciled with those for the entire RV examined in the present study. It was found that for the medium and high ranges of LVPL and RVPL, T of LV and RV were independent of the applied preloads; a dependence of T on preload was confirmed only for the low preload ranges. Thus, the results of this investigation may contribute to the understanding of RV myocardial relaxation, which has not yet been examined exhaustively at the level of the isolated entire RV.

Clinical implications and conclusions

Our findings are of clinical relevance insofar as, pathophysiologically, early stage LV dysfunction is considered to be compensated for indirectly by an adequate adaptation of RV activity. However, because the RV's ability to respond to acute changes in loading conditions, such as by shortening of T, has been shown to be very limited, it may be doubted whether reliance on RV compensation is justified.

In summary, LV and RV performances displayed coexisting analogies, similarities and dissimilarities. In the case of relaxation, a concept that quantitatively unifies the heterogeneous sets of data for both ventricles has been developed. Such a concept may guide future research; for example, the hypothesis may be put forward that reference was made to known mechanisms of cellular calcium handling.

The results of this investigation contribute to the understanding of RV myocardial relaxation at the level of the isolated entire RV. The coexistence of functional similarities and differences may render recent clinical findings more comprehensive (7,8) or add to the sparse unilateral experimental research on the RV (39).

REFERENCES

1. Langendorff O. Untersuchungen am überlebenden Säugethierherzen. Pflügers Arch Gesamte Physiol 1895;61:291-332.
2. Morgan HE, Neely JR, Wood RE, Liébecq C, Liebermeister H, Park CR. Factors affecting glucose transport in heart muscle and erythrocytes. Fed Proc 1965;24:1040-5.
3. Werchan PW, McDonough KH. The right ventricular working heart preparation. Proc Soc Exp Biol Med 1987;185:339-49.
4. Kolar F, Ostadal B. Right ventricular function in rats with hypoxic pulmonary hypertension. Pflügers Arch 1991;419:121-6.
5. Demmy TL, Magovern GJ, Kao RL. Isolated biventricular working rat heart preparation. Ann Thorac Surg 1992;54:915-20.
6. Itoi T, Lopachuk GD. Calcium improves mechanical function and carbohydrate metabolism following ischemia in isolated biventricular working hearts from immature rabbits. J Mol Cell Cardiol 1996;28:1501-14.
7. Bowers TR, O'Neill WW, Grines C, Pica MC, Safian RD, Goldstein JA. Effect of reperfusion on biventricular function and survival after right ventricular infarction. N Engl J Med 1998;338:933-40.
8. Geva T, Powell AJ, Crawford EC, Chung T, Colan SD. Evaluation of regional differences in right ventricular systolic function by acoustic quantification echocardiography and cine magnetic resonance imaging. Circulation 1998;98:339-45.
9. Irlbeck M, Mühling O, Iwai T, Zimmer H-G. Different response of the rat left and right heart to norepinephrine. Cardiovasc Res 1996;31:157-62.
10. Zimmer H-G, Gerdes AM, Lortet S, Mall G. Changes in heart function and cardiac cell size in rats with chronic myocardial infarction. J Mol Cell Cardiol 1990;22:1231-43.
11. Bünger R, Haddy FJ, Querengässer A, Gerlach E. An isolated guinea pig heart preparation with in vivo like features. Pflügers Arch 1975;353:317-29.
12. Taegtmeyer H, Hems R, Krebs HA. Utilization of energy-providing substrates in the isolated working rat heart. Biochem J 1980;186:701-11.
13. Müller-Strahl G, Kottenberg K, Zimmer H-G, Noack E, Kojda G. Inhibition of nitric oxide synthase augments the positive inotropic effect of nitric oxide donors in the rat heart. J Physiol 2000;522:311-20.
14. Westerhof N, Elzinga G, Sipkema P. An artificial arterial system for pumping hearts. J Appl Physiol 1971;31:776-81.
15. Glower DD, Spratt JA, Snow ND, et al. Linearity of the Frank-Starling relationship in the intact heart: the concept of preload recruitable stroke work. Circulation 1985;71:994-1009.
16. Yamagushi S, Li KS, Harasawa H, Zhu D, Santamore WP. The left ventricle affects the duration of right ventricular ejection. Cardiovasc Res 1993;27:211-5.
17. Elzinga G, Piene H, De Jong JP. Left and right ventricular pump function and consequences of having two pumps in one heart. A study on the isolated cat heart. Circ Res 1980;46:564-74.
18. Elzinga G, Westerhof N. How to quantify pump function of the heart. The value of variables derived from measurements on isolated muscle. Circ Res 1979;44:303-8.
19. Bünger R, Sommer O, Walter G, Stiegler H, Gerlach E. Functional and metabolic features of an isolated perfused guinea pig heart performing pressure-volume work. Pflügers Arch 1979;380:259-66.
20. Piene H, Sund T. Flow and power output of right ventricle facing load with variable input impedance. Am J Physiol 1979;237:H125-30.
21. Gillebert TC, Leite-Moreira AF, De Hert SG. The hemodynamic manifestation of normal myocardial relaxation. Acta Cardiol 1997;52:223-46.
22. Starling EH, Visscher MB. Regulations of energy output of the heart. J Physiol 1926;62:243-61.
23. Frank O. On the dynamics of cardiac muscle. Am Heart J 1959;58:282-317 and 467-478.
24. Weber KT, Janicki JS, Reeves RC, Hefner LL, Reeves TJ. Determinants of stroke volume in the isolated canine heart. J Appl Physiol 1974;37:742-7.
25. Weber AM, Murray JM. Molecular control mechanisms in muscle contraction. Physiol Rev 1973;53:612-73.
26. Gillebert TC, Leite-Moreira AF, De Hert SG. Relaxation-systolic pressure relation. A load independent assessment of the left ventricular contractility. Circulation 1997;95:745-51.
27. Imperial ES, Levy MN, Zieske H Jr. Outflow resistance as an independent determinant of cardiac performance. Circ Res 1961;9:1148-55.
28. Rosenfeldt FL, Cobb FR, Bache RJ, Sabiston DC Jr. Effect of increases in afterload before and after coronary occlusion in awake dogs. Cardiovasc Res 1979;13:392-400.
29. Mahler F, Ross J Jr, O'Rourke RA, Covell JW. Effects of changes in preload, afterload and inotropic state on ejection and isovolumic phase measures of contractility in the conscious dog. Am J Cardiol 1975;35:626-34.
30. Lew WYW. Asynchrony and ryanodine modulate load-dependent relaxation in the canine left ventricle. Am J Physiol 1995;268:H17-24.
31. Brutsaert DL, de Clerk NM, Goethals MA, Housmans PR. Relaxation of ventricular cardiac muscle. J Physiol 1978;283:469-80.
32. Dillmann WH. Calcium regulatory proteins and their alteration by transgenic approaches. Am J Cardiol 1999;83:89-91.
33. Gupta RC, Mishra S, Mishima T, Goldstein S, Sabbah HN. Reduced sarcoplasmatic reticulum Ca(2+)-uptake and expression of phospholamban in left ventricular myocardium of dogs with heart failure. J Mol Cell Cardiol 1999;31:1381-9.
34. Capasso JM, Puntillo E, Olivetti G, Anversa P. Differences in load dependence of relaxation between the left and right ventricular myocardium as a function of age. Circ Res 1989;65:1499-507.

35. Pouleur H, Lefèvre J, Van Mechelen H, Charlier AA. Free wall shortening and relaxation during ejection in the canine right ventricle. Am J Physiol 1980;239:H601-13.
36. Housmans PR, Murat I. Comparative effects of halothane, enflurane, and isoflurane at equipotent anesthetic concentrations on isolated ventricular myocardium of the ferret: II. Relaxation. Anesthesiology 1988;69:464-71.
37. Lecarpentier YL, Chemla D. Mechanical analysis of sarcomeres by laser diffraction: energy exchange and cardiac insufficiency. In: Swynghedauw B, ed. Research in Cardiac Hypertrophy and Failure. London: INSERM, 1990:137-60.
38. Zile MR, Conrad CH, Gaasch WH, Robinson KG, Bing OHL. Preload does not affect relaxation rate in normal, hypoxic, or hypertrophic myocardium. Am J Physiol 1990;258:H191-7.
39. Scherrer-Crosbie M, Steudel W, Hunziker PR, et al. Determination of right ventricular structure and function in normoxic and hypoxic mice. A transesophageal echocardiographic study. Circulation 1998;98:1015-21.